THE JOURNAL OF PHYSICAL CHEMISTRY B

Article

pubs.acs.org/JPCB

Conformational Properties of Sodium Polystyrenesulfonate in Water: Insights from a Coarse-Grained Model with Explicit Solvent

Sriteja Mantha and Arun Yethiraj*

Theoretical Chemistry Institute, Department of Chemistry, University of Wisconsin, 1101 University Avenue, Madison, Wisconsin 53706, United States

Supporting Information

ABSTRACT: Polymer solutions present a significant computational challenge because chemical realism on small length scales can be important, but the polymer molecules are very large. In polyelectrolyte solutions, there is often the additional complexity that the molecules consist of hydrophobic and charged groups, which makes an accurate treatment of the solvent, water, crucial. One route to achieve this balance is through coarse-grained models where several atoms on a monomer are grouped into one interaction site. In this work, we develop a coarse grained (CG) model for sodium polystyrenesulfonate (NaPSS) in water using a methodology consistent with the MARTINI coarse-graining philosophy, where four heavy atoms are grouped into one CG site. We consider two models for water: polarizable MARTINI (POL) and big multipole water (BMW). In each case, interaction parameters for the polymer sites are obtained by matching the potential of mean force between two monomers to results of atomistic simulations. The force field based on the POL water provides a more reasonable description of polymer properties than that based on the BMW water. We study the properties of single chains using the POL force field. Fully sulfonated chains are rodlike (i.e., the root-mean-square radius of gyration, R_g, scales linearly with degree of polymerization, N). When the fraction of sulfonation, f, is 0.25 or less, the chain collapses into a cylindrical globule. For $f = 0.5$, pearl-necklace conformations are observed when every second monomer is sulfonated. The lifetime of a counterion around a polymer is on the order of 100 ps, suggesting that there is no counterion condensation. The model is computationally feasible and should allow one to study the effect of local chemistry on the properties of polymers in aqueous solution.

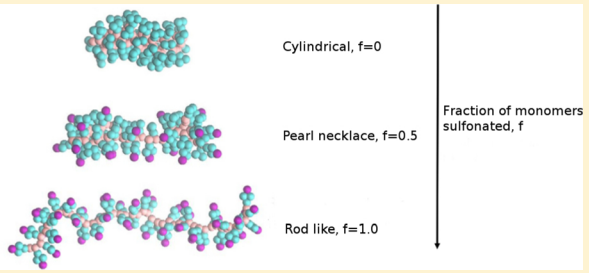

1. INTRODUCTION

Polyelectrolyte solutions have fascinating physical properties and wide-ranging applications and are still considered one of the least understood systems in soft matter.[1−8] The most widely studied synthetic polymer is probably sodium polystyrenesulfonate (NaPSS). This molecule has a hydrophobic backbone and is soluble because of the charged side groups, and the physical properties are the result of a balance between these interactions. It might therefore be expected that the local chemical details could be important for an understanding of their solution behavior.

The vast majority of theoretical and computational work, on the other hand, has focused on generic charged bead−spring models for the poly ions.[9−15] These studies have provided considerable insight into the universal properties. The shortcomings of generic models have been emphasized,[16−18] especially the importance of explicit solvent on the qualitative behavior of polyelectrolyte solutions in the bulk and at surfaces. It is of interest therefore to investigate the effect of local chemistry on the properties of polyelectrolyte solutions.

Atomistic simulations of polyelectrolyte solutions are challenging for a number of reasons. Park et al.[19] performed single chain simulations of NaPSS in water and showed that standard molecular dynamics simulations did not sample configurational space, and computationally intensive Hamiltonian replica exchange simulations were necessary. This greatly restricted the size of the systems they could study, namely single chains with degree of polymerization $N \leqslant 16$, compared to the range $40 \leqslant N \leqslant 700$ studied experimentally. Other atomistic simulations either use implicit solvent or study short chains.[20−22]

An attractive middle ground is the use of coarse-grained (CG) models of polymers. A popular model in biophysics is the MARTINI CG force field,[23] where 2−4 heavy atoms are grouped into a single interaction site, and four water molecules are grouped into a single water site. This mapping is chosen so that all the sites have the same diameter, which results in an enormous computational savings. These CG simulations are several orders of magnitude faster than atomistic simulations and have a much smoother free-energy landscape. CG models for poly(ethylene oxide) and polystyrene have been reported in the literature.[24−26] There is one CG model for polystyrenesulfonate,[27] which uses an implicit solvent. In this work, we

Special Issue: Biman Bagchi Festschrift

Received: February 19, 2015
Revised: June 5, 2015
Published: June 5, 2015

DOI: 10.1021/acs.jpcb.5b01700
J. Phys. Chem. B 2015, 119, 11010−11018

develop a CG model for NaPSS, with explicit solvent, based on the MARTINI approach.

We develop CG force fields with two different water models, the polarizable MARTINI (POL)[28] and the big multipole water (BMW).[29] The bond angle and bond length potentials are obtained by fitting these potentials to atomistic simulations of a single chain and the nonbonded interactions are obtained by attempting to reproduce atomistic simulation results for the potential of mean force between two monomers in water. We find that the force field based on the POL model is in good agreement with atomistic simulations for the end-to-end distance potential of mean force in a single polymer chain and recommend its use for NaPSS simulations.

Simulations with the CG model show that a single chain is stretched when the polymer is fully sulfonated, and collapses into a cylinder when the polymer has a low fraction of sulfonated monomers. For intermediate degrees of sulfonation, the conformational properties are a strong function of the sequence (i.e., the location of the sulfonated monomers along the chain backbone). We see no evidence for counterion localization, or condensation, even though the counterions have strong structural correlations with the polymer sites.

The rest of the paper is organized as follows. Details on model development are presented in section 2, simulation details are reported in section 3, results are presented and discussed in section 4, and conclusions from this work are presented in section 5.

2. MODEL DEVELOPMENT

2.1. Coarse-Grained Model and Bonded Interactions.

Our coarse grained model for polystyrenesulfonate is based on the MARTINI type model for polystyrene developed by Rossi et al.[26] As shown in Figure 1, each monomeric unit is mapped

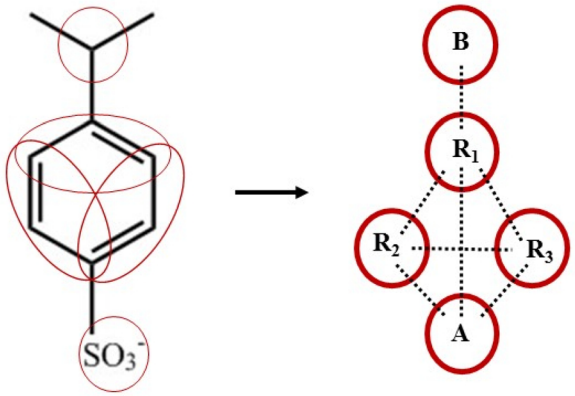

Figure 1. Coarse-grain mapping scheme. In the CG model, B represents backbone bead, R_i represents ring bead, and A represents sulfonate bead.

on to a 5 site model with three sites (R_1, R_2, and R_3) for the benzene ring, one (A) for the sulfonate group, and one (B) for the backbone groups composing the CH group and the neighboring CH_2 group. The negative charge on the CG monomer is distributed on the R_2 (−0.2e), R_3(−0.2e), and A(−0.6e) beads. These partial charges are based on the corresponding charges of the constituent atoms in the atomistic model. All monomers are identical (i.e., we do not treat the end groups differently).

The potential energy of the system is the sum of bonded and nonbonded interactions. For simplicity, we include only bond length and bond angle potentials (i.e., no dihedral angle potential) in the bonded interactions. Our model therefore cannot capture the properties associated with the tacticity of the polymer. The bond length between the backbone beads is flexible, with a bonding potential given by

$$U_b(x) = \frac{1}{2}K_b(x - x_0)^2 \quad (1)$$

where x is the length of the bond, and K_b and x_0 are constants. A bond angle potential is included for the bond angle between the backbone bead and other beads. This potential is given by

$$U_\theta(\theta) = \frac{1}{2}K_\theta(\theta - \theta_0)^2 \quad (2)$$

where θ is the bond angle and K_θ and θ_0 are constants. The parameters K_b, x_0, K_θ, and θ_0 are obtained from the work of Rossi et al.[26] on polystyrene (i.e., K_b = 8000 kJ mol^{-1} nm^{-2}, x_0 = 0.25 nm), and the values for the bond angle potentials are listed in Table 1. The bond length $B-R_1$ is fixed at 0.217 nm following Rossi et al.[26]

Table 1. Values for Bond Angle Parameters in the Coarse-Grained Model

angle	K_θ (kJ mol^{-1} rad^{-2})	θ_0 (degrees)
$B-R_1-R_1$	200	156
$R_i-B_j-B_k$	45	125
B−B−B	25	170

Other bonds are kept rigid, and the lengths are obtained from the bond probability distribution function in atomistic simulations. Within the MARTINI CG framework, a benzene ring is represented by three beads connected in a triangular fashion, with the bond length between these beads (R_i-R_j in our model) constrained to a value of 0.27 nm.[30] This approach allows one to preserve the planarity of the benzene ring. We add an additional bead (anion bead A) to represent the sulfonate group. The bond lengths R_2-A and R_3-A are constrained to 0.27 nm, and the bond length R_1-A is constrained to 0.47 nm. The latter is necessary to keep the anion bead in the same plane as the styrene group. The bond lengths used are listed in Table 2

Table 2. Values of Bond Lengths of the Rigid Bonds in the Coarse-Grained Model

bond	length (nm)
$B-R_1$	0.217
R_i-R_j	0.27
R_1-A	0.47
R_2-A	0.27
R_3-A	0.27

2.2. Nonbonded Interactions.

Nonbonded interactions are represented by the sum of Lennard-Jones (LJ) 12-6 potential given by

$$U_{LJ}(r) = 4\epsilon_{ij}\left[\left(\frac{\sigma_{ij}}{r}\right)^{12} - \left(\frac{\sigma_{ij}}{r}\right)^{6}\right] \quad (3)$$

DOI: 10.1021/acs.jpcb.5b01700
J. Phys. Chem. B 2015, 119, 11010−11018

Table 3. Nonbonded Interaction Parameters That Were Adjusted by Comparing the PMF between Monomers in CG Simulations to That Obtained from Atomistic Simulations

	POL			BMW		
	initial	final	% change	initial	final	% change
interaction type	ϵ (kJ/mol)	ϵ (kJ/mol)	δ	ϵ (kJ/mol)	ϵ (kJ/mol)	δ
R−W	2.565	3.325	29.63	1.916	2.201	14.87
B−W	1.9	2.184	14.95	1.420	1.633	15.00
R−A	–	–	–	4.000	3.500	12.50

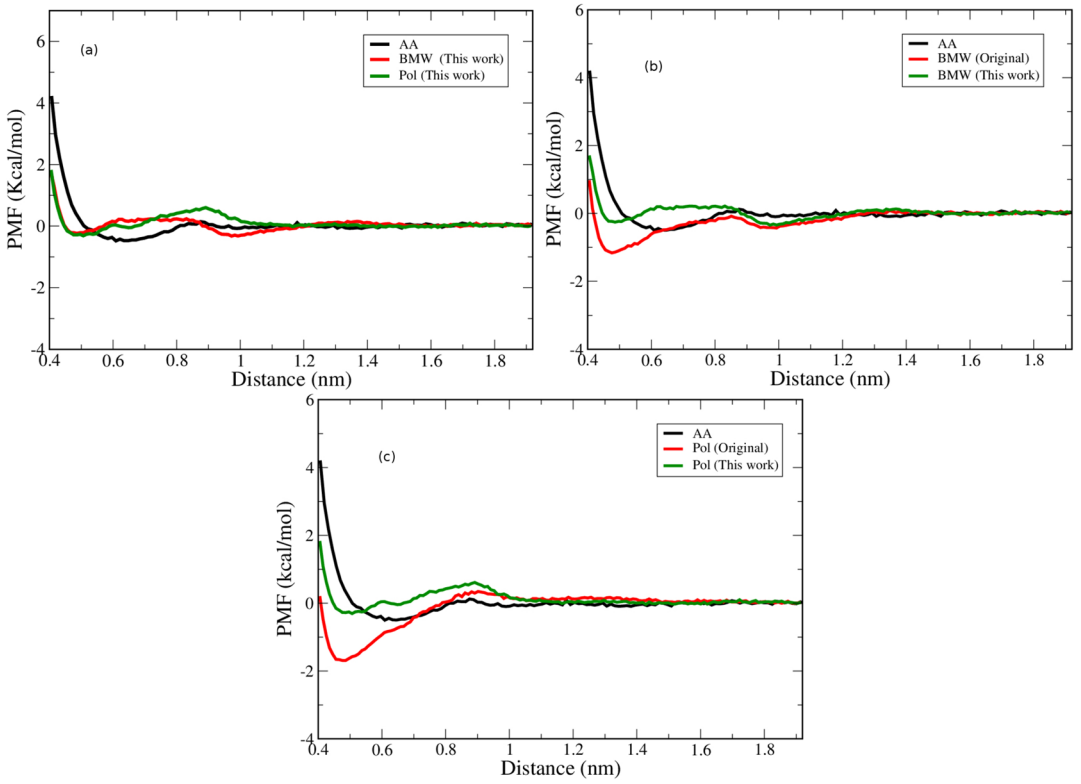

Figure 2. Potential of mean force between two monomers in water. The symbols AA, BMW, and POL refer to the atomistic model, CG model with POL water, and CG model with BMW water, respectively. (a) Depiction of the final parameter set for the POL and BMW models compared to the atomistic result. (b) and (c) Comparison, for the BMW and POL models, respectively, of the PMF obtained from the original CG force field and the force field developed in this work, to atomistic simulations.

where σ_{ij} and ϵ_{ij} are the collision diameter and well depth between sites i and j, and a Coulomb potential (for charged groups).

The starting point is the choice of a CG water model, and we consider two models: the polarizable Martini (POL)[28] and Big Multipole Water (BMW) models,[29] both of which consider the electrostatic properties of the solvent and are designed to represent four water molecules. For each of these models, we develop a force field for the PSS monomer. For an initial guess, we use the parameters from the POL and BMW/MARTINI force fields.[30,31] In particular, we assign type SC1 for the backbone bead, SC4 for the ring beads, and Qa for the bead representing sulfonate group.

The LJ parameters are then adjusted to reproduce atomistic simulation results for the potential of mean force (PMF) between monomers in water, where the reaction coordinate is the separation between R_1 sites on different monomers. We choose to parametrize based on atomistic simulations because experimental results are not available for single chains. As a caveat, it is not obvious that this will faithfully reproduce experimental results for semidilute and concentrated solutions (i.e., the transferability of the potential remains an open question). Using the POL and BMW estimates for these parameters gives a PMF that is far too attractive (i.e., the solvent is too poor). Therefore, one would require either stronger polymer−water interactions or weaker polymer−polymer interactions.

The Lennard-Jones parameters are obtained by adjusting four (of the ten) pair interactions: B−W, R−W, R−A, and B−A, where B, W, R, and A refer to sulfonate (A), backbone (B), ring (R), and water (W) sites, respectively. We do not adjust the interaction between two identical sites (e.g., R−R, because these have been fit to the thermodynamic properties of individual solutes). To keep the model for polystyrenesulfonate consistent with that for polystyrene we do not alter the B−R interaction, and we do not adjust the A−W interaction because it is already attractive, and decreasing this strength will decrease the solvent quality.

The MARTINI CG force field prescribes four main types of interaction sites, namely, polar (P), nonpolar (N), apolar (C), and charged (Q). Each of these types are further divided into subtypes depending on their hydrogen-bonding capabilities (d

DOI: 10.1021/acs.jpcb.5b01700
J. Phys. Chem. B 2015, 119, 11010−11018

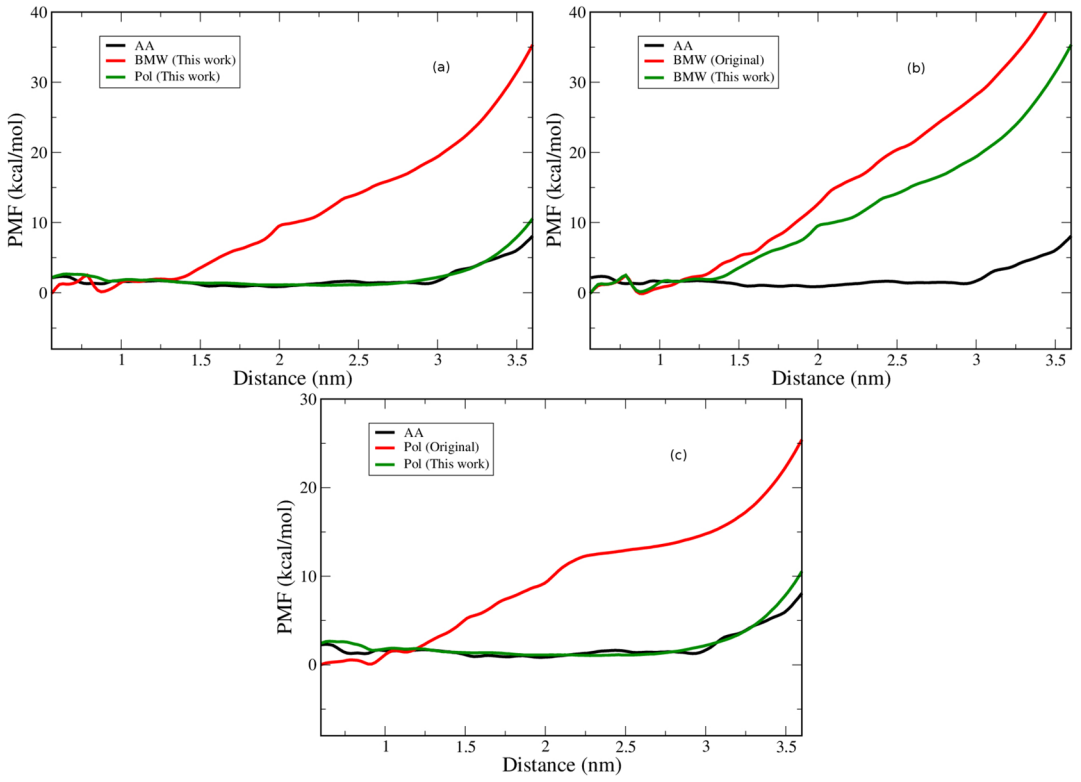

Figure 3. End-to-end potential of mean force of fully sulfonated NaPSS in water. The symbols AA, BMW, and POL refer to the atomistic model, CG model with POL water, and CG model with BMW water, respectively. (a) Depiction of the final parameter set for the POL and BMW models compared to the atomistic result. (b) and (c) Comparison, for the BMW and POL models, respectively, the PMF obtained from the original CG force field and the force field developed in this work, to atomistic simulations.

= donor, a = acceptor, da = both, and 0 = none) or by a number indicating the degree of polarity (from 1, low polarity, to 5, high polarity). Within the MARTINI CG framework, LJ interactions between different CG bead types are classified into different levels of interaction, with the interaction strength ranging from 5.6 kJ/mol for most polar interaction to 2.0 kJ/mol. On the basis of this prescription and following Rossi et al. work on the CG model for polystyrene,[26] we assign initial values to the CG parameters [i.e., we assign type SC1 for the backbone bead, SC4 for the ring bead, Qa for the sulfonate bead, and Qd for the sodium counterion (Na^+)].

We then adjust the four parameters by sequentially increasing or decreasing the interaction level by one. If the change improves the agreement with atomistic simulations, we accept it, otherwise, we keep the previous parameters. Details regarding the parametrization are presented in the Supporting Information. For the parameters that change, the initial and final values are listed in Table 3.

Figure 2 compares the final CG potential of mean force (PMF) between two monomers in atomistic simulations. The CG models provide a reasonable description of the PMF, within 0.5 kcal/mol at all separations, although there are some systematic differences. The first minimum in the PMF occurs at a smaller separation (0.5 nm) in the CG models than in the atomistic model (where it occurs at 0.75 nm). The POL model overestimates the magnitude of the peak at 0.9 nm, while the BMW model appears to have a shallow solvent-separated minimum in the PMF at a distance of 1 nm. We attribute the lack of quantitative agreement between CG and atomistic models to the nature of the CG models rather than the value of the parameters.

The somewhat poor agreement between the CG models and atomistic simulations for the monomer−monomer PMF is disappointing. Of particular concern is the fact that the positions of the minima are different in the CG models when compared to the atomistic simulations. These qualitative features are sensitive to the form of the interactions rather than values of the parameters, and it is possible that it will not be possible with these models to reproduce the monomer−monomer PMF accurately. We therefore use a polymer related quantity, the end-to-end distance PMF, to justify the choice of model.

2.3. Force Field Validation. The POL model is in excellent agreement with atomistic simulations for the PMF between the ends of a fully sulfonated PSS chain. Figure 3 depicts the PMF between the two ends of a 16-mer, where the reaction coordinate is the distance between the end carbon atoms to which the ring groups are attached. The discrepancies occur at short distances, where atomistic details are expected to be important and at long distances where chain stretching in the POL model can come only from bond extension as opposed to dihedral rotations in the atomistic model. The BMW model is in very poor agreement with the atomistic simulations for the PMF and predicts a rapid increase in the free energy at distances greater than 1.4 nm. From this test, we conclude that the POL model provides a reasonable description of single chain properties, but the BMW model does not, and the POL model is used for more extensive simulation studies.

The BMW model predicts a large increase in the free energy with increasing end-to-end distance, and a reparameterization does not have a significant effect. We speculate that this is because the water−water interactions in BMW are too

DOI: 10.1021/acs.jpcb.5b01700
J. Phys. Chem. B 2015, 119, 11010−11018

favorable compared to the water−polymer interactions. In the BMW/MARTINI model a soft Born-Mayer-Huggins non-electrostatic interaction potential is used between the water molecules, but a Lennard-Jones interaction is used between all other sites. This makes the polymer too hydrophobic and the charged polyelectrolyte collapses in dilute solution! As a consequence, the free energy required to pull the chain into an extended conformation is very high. This effect is accentuated by the fact that, in addition to the first minimum, there is a solvent-separated minimum in the monomer−monomer PMF, making the propensity to collapse the chain greater. We attribute the success of the BMW/MARTINI model for lipid/peptide mixtures[32,33] to the fact that the hydrophobic and hydrophilic regions are spatially separated due to self-assembly (into bilayers or bicontinuous phases). The BMW/MARTINI model is less successful for polymers, where the balance between these interactions is more subtle.

3. SIMULATION DETAILS

We perform three types of simulations: simulations of molecules in water, the PMF between two monomers in water, and the end-to-end distance PMF of a single polymer chain in water. All simulations are carried out using GROMACS 4.5.4[34] simulation package. The simulation cell is a cube with periodic boundary conditions in all directions.

For simulations of molecules in water, initial configurations are generated by first inserting a solute molecule into the cubic simulation box and then adding solvent molecules. For chains with fewer than 16 monomers, initial configurations are created with the chains in an extended conformation. For longer chains, equilibrated final configurations of two shorter chains are selected, and the desired chain length is obtained by connecting these shorter chains at one end.

Atomistic simulations are performed using the CHARMM based force field used by He et al.[35] in their simulations of linear alkyl benzenesulfonates at air water interface. This force field has also been used by Park et al.,[19] for simulations of dilute solutions of PSS. A cutoff of 1.4 nm is used for nonbonded Lennard-Jones interactions, and Coulomb interactions are handled with the particle mesh Ewald method (PME)[36,37] method. The PME parameters are as follows: real space cutoff distance of 1.4 nm and interpolation order of 6 with a maximum fast Fourier transform grid spacing of 0.12 nm. Bond lengths in the solute molecule are constrained using the LINCS algorithm[38] and the water molecules are kept rigid using the SETTLE algorithm. Temperature and pressure are maintained using a Nose-Hoover thermostat[39,40] (coupling time 0.5 ps) and Parinello-Rahman barostat[41] (coupling time 1 ps). The TIP3P model is used for water, and the simulations are carried out with an integration time-step of 2 fs.

The protocol for the simulations of CG systems is as prescribed by the developers of the force field(s). In the POL model, the cutoff distance for the Lennard-Jones interaction is 1.2 nm with a smooth decay to zero between 0.9 and 1.2 nm. Electrostatic interactions are calculated by using PME method with a spacing of 0.2 nm, a real space cutoff distance of 1.4 nm and a dielectric constant $\epsilon_r = 2.5$. The LINCS algorithm is used to constrain all bonds. In simulations with the BMW model, a switch scheme (r_{switch} =1.2 nm and r_{cut} = 1.4 nm) is used for water−water interactions, and the shift cutoff scheme as that of the POL model is used for all other Lennard-Jones interactions. The PME method with a spacing of 0.2 nm, a real space cutoff distance of 1.4 nm and a dielectric constant $\epsilon_r = 1.3$, is used for the electrostatic interactions. The SETTLE algorithm is used to constrain bonds in CG water, and LINCS is used for all the other bonds. In both the models, Berendsen's thermostat and barostat are used to maintain constant temperature and pressure conditions, respectively. Simulations are carried out with integration time step of 20 fs.

Starting with the initial configuration, the energy of the system is first minimized using the steepest descent method and the resulting configuration is equilibrated for 25 ns at 350 K and 1 bar in the isobaric−isothermal ensemble. Simulations are then performed under constant NVT ensemble conditions at 300 K with an initial equilibration period of about 50 ns. Equilibration time considered in our CG simulations under constant NVT ensemble conditions is approximately five times the time taken for the solute end-to-end vector autocorrelation function to decay to zero. Properties are averaged over roughly one microsecond.

The PMF between two monomers in water is obtained using umbrella sampling. We define the primary atom on each molecule as the R_1 site in the CG case and the ring carbon atom connected to the backbone in the atomistic case. The reaction coordinate is the distance between primary atoms. Initial conditions are created by placing the two molecules with a reaction coordinate distance of 2 nm in a cubic box of edge length 6 nm. The molecules are solvated with water molecules and sodium counterions as described above. The energy is minimized, and the system equilibrated at 350 K and 1 bar with the distance between primary carbon atoms constrained to be 2 nm. The system is then further equilibrated at 300 K under constant NVT conditions. The force constant for the umbrella bias potential is 1000 kJ/mol nm^2, and 40 windows are used for the reaction coordinate varying from 2 to 0.4 nm where the windows are spaced by 0.04 nm. The initial conditions for each window are obtained from the initial configuration at 2 nm by pulling the solute molecules to the desired separation using the pull code in the GROMACS package. These initial configurations are equilibrated at 300 K under constant NVT ensemble conditions. The reaction coordinate is constrained during equilibration. The equilibrated structure at each window is then used to carry out long simulations at 300 K under constant NVT conditions.

For the atomistic simulations, the system at each window is equilibrated for 1.5 ns, followed by a production run of 15 ns. The trajectories are recorded for every 1000th step and the last 10 ns of trajectory at each window is used to calculate PMF. For the CG simulations, the system at each window is equilibrated for 5 ns, followed by a production run of 100 ns. The trajectories are recorded for every 5000th step, and the last 80 ns of trajectory at each window is used to calculate PMF. This combination of simulation time, force constant, and window spacing for umbrella sampling simulations has given us histograms with reasonable overlap. The PMF is obtained using the WHAM algorithm.[42,43]

The end-to-end distance PMF is obtained using umbrella sampling. In the atomistic model, the reaction coordinate is the distance between the carbon atoms of the methylated end groups, and in the CG models, the reaction coordinate is the distance between the terminal backbone beads. The force constant for the bias potential is set to 1000 kJ/mol nm^2, and 36 windows with reaction coordinate ranging from 0.4 to 4.0 nm with a window spacing of 0.1 nm are used. (A fully extended 16-mer PSS chain has an end-to-end distance of approximately 4 nm). Umbrella sampling simulations are

DOI: 10.1021/acs.jpcb.5b01700
J. Phys. Chem. B 2015, 119, 11010−11018

carried out in a cubic box of edge length 8 nm. Initial configurations for each window are generated from extended conformation of 16-mer PSS chain. Simulation protocol employed to compute PMF as a function of end-to-end distance is similar to that described for the two monomer PMF calculations.

4. RESULTS AND DISCUSSION

The results presented here are all with the POL model, which is in reasonably good agreement with atomistic simulations for the end-to-end distance PMF. Simulations with the POL model are not plagued by the sampling issues seen in atomistic simulations. For 16-mers, the end-to-end vector autocorrelation function decays to zero within 10 ns, and the correlation length (i.e., the time it takes for this autocorrelation function to decay to 1/e its value at $t = 0$) is approximately 1 ns. Furthermore, the distribution of end-to-end distance and radius of gyration obtained from independent simulations are almost indistinguishable (within statistical uncertainties). We are therefore confident that the simulations sample configurational space adequately. However, long simulations (microseconds) are necessary to obtain a sufficiently large number of independent conformations.

4.1. Conformational Properties. Fully sulfonated chains display rodlike scaling. For N = 16, 24, 32, 40, 48, 56, and 64, $R_g = 0.05N$ provides an excellent fit for the simulation results. The distribution of R_g is different in CG and atomistic simulations, although the average value is similar. Figure 4

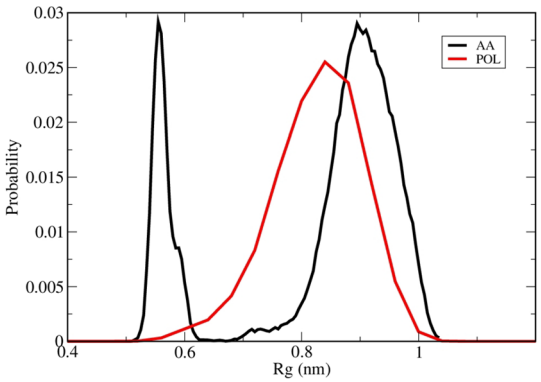

Figure 4. Comparison of the distribution of radius of gyration of fully sulfonated 16-mers at 300 K obtained from the POL model to atomistic simulations.[19]

compares POL results for the distribution of radius of gyration of a fully sulfonated 16-mer to atomistic simulations results of Park et al.[19] The distribution function has only one peak in the CG model but two peaks in the automatic model, although the average value of R_g is the same in both cases. It is not clear which model is correct because the atomistic simulations are plagued by sampling issues, and the CG model is not expected to reproduce behavior at short length scales. Experiments would be required to resolve this discrepancy.

If one excludes the first peak in the AA distribution, the POL model appears to predict a distribution of sizes that is slightly smaller than the AA result. Although it is consistent with the minimum in the monomer−monomer PMF being at shorter distances in the POL model (see Figure 2), it is more likely due to the solvent structure around the polyion. This is because the correlation between R_1 sites (when monomers are connected into a chain) is dominated by intramolecular bonding interactions, which keep these sites at distances larger than the minimum in the PMF (see Figure 6).

As the degree of sulfonation is decreased, the chain collapses, and uncharged chains take on a cylindrical conformation. Figure 5 depicts the radius of gyration of the backbone as a

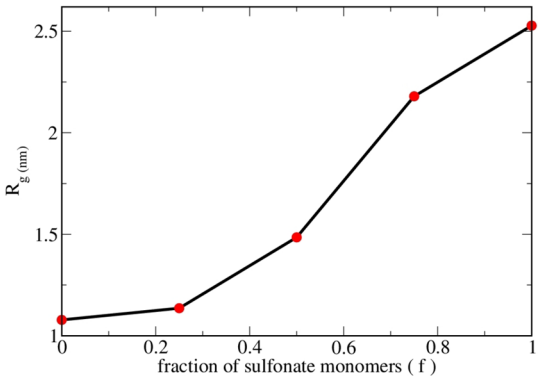

Figure 5. Radius of gyration computed from backbone beads as a function of degree of sulfonation for N = 48.

function of degree of sulfonation f for N = 48. The chains are uniformly sulfonated (i.e., for f = 0.25 and 0.5, every fourth and second monomer is sulfonated, and for f = 0.75, every fourth monomer is not sulfonated). For f = 0, the chain is collapsed and for larger values of f, R_g increases monotonically as f is increased.

Representative snapshots of the final configuration are depicted in Figure 6. Note that the shape of the polymer is

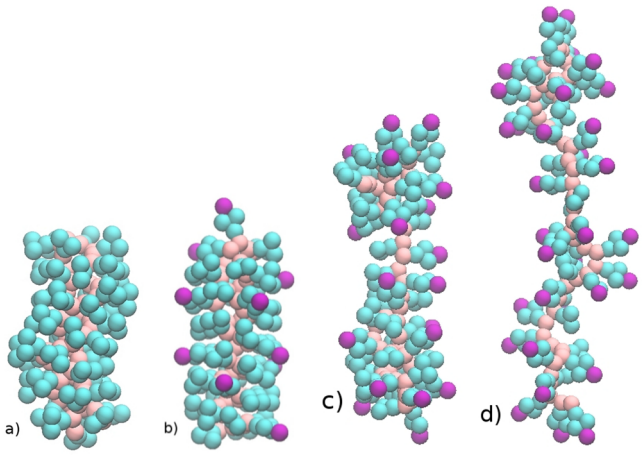

Figure 6. Represenative simulation snapshots of the polymer molecule with N = 48 and (a) f = 0. (b) f = 0.25, (c) f = 0.5, and (d) f = 0.75.

cylindrical rather than spherical for f = 0, which arises from the bulky styrene groups. For f = 0.5, the chain displays the pearl-necklace conformation predicted by Dobrynin et al.[44] To our knowledge, this structure has not been previously observed in simulations with explicit solvent and chemical detail. As f is increased further, the chain becomes extended.

The single chain static structure factor is a good measure of the conformational properties. Figure 7 depicts the structure factor in standard Kratky form, $q^2P(q)$ vs q, where $P(q)$ is the structure factor, and is computed from

DOI: 10.1021/acs.jpcb.5b01700
J. Phys. Chem. B 2015, 119, 11010−11018

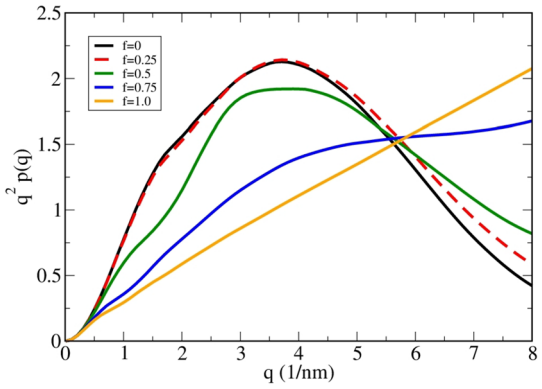

Figure 7. Kratky plot of the single chain structure factor as a function of degree of sulfonation for $N = 48$.

$$P(q) = \frac{1}{N^2}\langle \sum_{ij} \exp(iq.\, r_{ij})\rangle \tag{4}$$

where N is number of backbone beads in the polymer, r_{ij} is distance between beads, and $\langle ...\rangle$ denotes an ensemble average. Only backbone beads are used for this calculation. In the scaling regime, $P(q) \sim q^{-4}$ for a sphere, $P(q) \sim q^{-2}$ for a Gaussian chain, and $P(q) \sim q^{-1}$ for a rod. In a Kratky plot, a Gaussian chain shows a plateau, a collapsed chain shows a maximum and a rod shows an increasing function of q. From the figure, it is clearly seen that polymers with $f = 0$ and 0.25 have similar structure. For $f = 0.5$, the chain appears collapsed, but there is an extra bump in the Kratky plot that might be a signature of the pearl-necklace structure. For $f = 0.75$, the chain is almost Gaussian, and for $f = 1$, it is rodlike.

The conformational properties are sensitive to the position of the sulfonated groups. In addition to the uniformly sulfonated polymer (described above), we investigate a diblock polymer (first 24 monomers sulfonated) and 5 different sequences where the sulfonated groups are selected randomly, all for $f = 0.5$. Figure 8 depicts representative simulation snapshots of the molecules corresponding to the structure representing their most probable radius of gyration. In the diblock polymer, part of the chain corresponding to nonsulfonated monomers collapses into a globule and the rest of the chain comprising sulfonated monomers take up an extended conformation, as expected. For the randomly sulfonated polymers, the conformation is sensitive to the sequence and the pearl-necklace structure is observed only in some cases.

A direct comparison with the experiments is complicated by several factors. Our simulations are for infinitely dilute solutions and fairly short chains, while experiments are usually for semidilute solutions and much longer chains. It is known that interchain correlations are important in polyelectrolyte solutions, even in dilute solution, and is manifested by a strong "polyelectrolyte" peak in the structure factor. The position, q^*, of this peak scales with concentration as $q^* \sim c^{1/3}$ and $q^* \sim c^{1/2}$ in dilute and semidilute solutions, respectively.[2] Of course, the very presence of this peak suggests the solutions cannot be dilute (i.e., intermolecular correlations are significant), and simulations show that the chain size decreases with concentration in the dilute regime.[45,46] Most experiments on PSS are for semidilute solutions and for degrees of polymerization greater than 725.[47−51] One could bridge this gap between simulations and experiment with measurements of conformations and volumetric properties on shorter chains and simulations for semidilute solutions. In the mean time, we are not aware of experiments against which we could test the simulation results.

4.2. Counterion Distribution and Dynamics. An important concept in polyelectrolyte theory is that of counterion condensation. The original Manning theory[52] considered limiting laws for a long polymer with a contour length of L and P charged groups. When the charged groups are monovalent, the counterions are predicted to condense on the polymer when $\xi \equiv l_B/b \geqslant 1$, where l_B is the Bjrerrum length and $b = L/P$ is the linear charge density. For the CG model, $L = (N-1)\, x_0$, $P = fN$, $x_0 = 2.5$ Å, and $l_B = 7.5$ Å, and therefore $\xi \approx 3f$. One might therefore expect signatures of condensation for $f > 1/3$. We see strong correlations between the counterions and the sulfonate group but no localization of the counterions, for $f > 1/3$.

We calculate the counterion residence time near a sulfonate ion from the lifetime of a counterion−sulfonate complex. To this end, we define a function $\phi(t)$.

$$\phi(t) = [n(t + t_0)n(t)_0] \tag{5}$$

where $n(t) = 1$ if the counterion is within a distance of 7 Å (which corresponds to position of first minimum in the counterion sulfonate pair correlation function) from a sulfonate bead and zero otherwise. The function is then averaged over all the counterions and over the ensemble and initial times t_0. We find that this function decays to zero within a few ns and define a residence time, τ, as the time it takes for $\phi(t)$ to decay to $1/e$ its initial value.

Figure 9 depicts the sulfonate-counterion pair correlation function for $N = 48$ and various degrees of (uniform) sulfonation. There is a strong peak at 5 Å, which corresponds to the distance of closest approach of a counterion to the sulfonate group and another smaller peak at 9 Å. These peaks can be attributed to contact ion-pairs and solvent-separated ion pairs. The contact peak is strongest for $f = 1$ and decreases as f decreases; this peak is slightly more intense for $f = 0.5$ than that

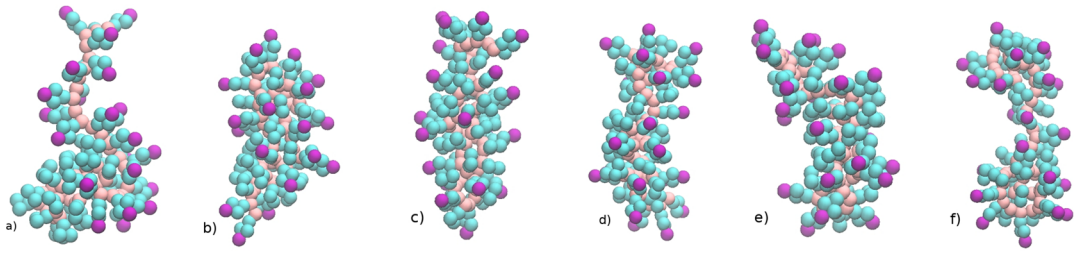

Figure 8. Representative snapshots of a polymer with 48 monomers and $f = 0.5$. (a) Structure with first 24 monomers sulfonated. (b−f) Sequences where sulfonated groups are randomly selected.

DOI: 10.1021/acs.jpcb.5b01700
J. Phys. Chem. B 2015, 119, 11010−11018

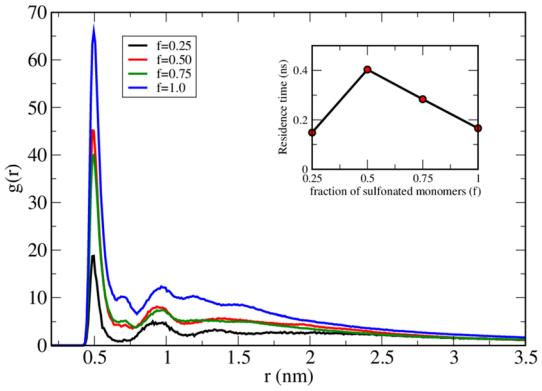

Figure 9. Counterion−sulfonate pair correlation function for $N = 48$ and various degrees of sulfonation.

for $f = 0.75$, which could be a manifestation of the pearl necklace conformation of polymer for this value of f. All cases except $f = 0.25$ are above the Manning condensation threshold. The inset of the figure shows the residence time τ. In all cases, τ is between 100 and 500 ps (i.e., the counterions are not localized near the sulfonate groups). τ is the smallest for $f = 0.25$, increases going from $f = 0.25$ to 0.5, and then decreases for larger values of f. The increase for $f = 0.5$ could be another signature of the existence of pearl-necklace conformations in polyelectrolytes.

5. CONCLUSION

We develop a coarse-grained model for polystyrenesulfonate. The model follows the MARTINI framework with four water molecules grouped into a single site. We follow the same procedure with the POL and BMW water models and find that the former gives results for the end-to-end distance PMF that are in better qualitative agreement with atomistic simulations. We therefore argue that this model is more appropriate and use it to study the properties of dilute solutions. The CG model does not suffer from the sampling issues we had encountered for atomistic models, and we are able to simulate longer chains and for longer times.

Uncharged chains are collapsed into cylindrical globules, and the chains expand as the degree of sulfonation is increased, if the sulfonation is uniform. Pearl-necklace conformations are observed when a fraction $f = 0.5$ monomers are sulfonated. The conformational properties are sensitive to the sequence of sulfonated monomers. For $f = 0.5$, the pearl-necklace conformations are only clearly observed if every alternate monomer is sulfonated. If half of the chain is sulfonated (as in a diblock copolymer), the sulfonated part takes an extended conformation where as the other half collapses into a globule, and if (half) the monomers are sulfonated randomly, the chain can adopt cylindrical conformations. Counterions are correlated with the polymer, as expected, but we do not observe any temporal localization (i.e., they are not condensed even for fully sulfonated chains).

The CG model presented here is promising because it incorporates significant chemical detail but does not suffer from the significant computational challenges of atomistic simulations. We anticipate that the model will provide a means of investigating the behavior of hydrophobic polyelectrolytes in semidilulte and concentrated solutions and provide physical insight that will enhance our understanding of polyelectrolyte solutions.

■ ASSOCIATED CONTENT

Supporting Information

Summary of the initial and final interaction parameters and also a description of the methodology employed to obtain interaction parameters for CG simulations of NaPSS in water. The Supporting Information is available free of charge on the ACS Publications website at DOI: 10.1021/acs.jpcb.5b01700.

■ AUTHOR INFORMATION

Corresponding Author

*E-mail: yethiraj@chem.wisc.edu.

Notes

The authors declare no competing financial interest.

■ ACKNOWLEDGMENTS

This research is supported by the National Science Foundation through Grant CHE-1111835. We are grateful for computational support through Extreme Science and Engineering Discovery Environment (XSEDE) allocations under Grant TG-CHE090065. We acknowledge the support from the UW-Madison chemistry department cluster under Grant CHE-0840494 and compute resources and assistance of the UW-Madison Center for High Throughput Computing (CHTC) . We also thank Dr. Soohyung Park for sharing with us different input files for setting up all atom simulations.

■ REFERENCES

(1) Barrat, J. L.; Joanny, J. F. Theory of polyelectrolyte solutions. *Adv. Chem. Phys.* **1996**, *94*, 1−66.
(2) Degennes, P. G.; Pincus, P.; Velasco, R. M.; Brochard, F. Remarks on polyelectrolyte conformation. *J. Phys. (Paris)* **1976**, *37*, 1461−1473.
(3) Dobrynin, A. V. Theory and simulations of charged polymers: From solution properties to polymeric nanomaterials. *Curr. Opin. Colloid Interface Sci.* **2008**, *13*, 376−388.
(4) Dobrynin, A. V.; Rubinstein, M. Theory of polyelectrolytes in solutions and at surfaces. *Prog. Polym. Sci.* **2005**, *30*, 1049−1118.
(5) Holm, C.; Joanny, J. F.; Kremer, K.; Netz, R. R.; Reineker, P.; Seidel, C.; Vilgis, T. A.; Winkler, R. G. Polyelectrolyte theory. *Adv. Polym. Sci.* **2004**, *166*, 67−111.
(6) Volk, N.; Vollmer, D.; Schmidt, M.; Oppermann, W.; Huber, K. Conformation and phase diagrams of flexible polyelectrolytes. *Adv. Polym. Sci.* **2004**, *166*, 29−65.
(7) Kuhn, P. S. Flexible polyelectrolytes in salt-free solutions. *Phys. A* **2004**, *337*, 481−494.
(8) Forster, S.; Schmidt, M. Polyelectrolytes in solution. *Adv. Polym. Sci.* **1995**, *120*, 51−133.
(9) Shew, C. Y.; Yethiraj, A. Computer simulations and integral equation theory for the structure of salt-free rigid rod polyelectrolyte solutions: Explicit incorporation of counterions. *J. Chem. Phys.* **1999**, *110*, 11599−11607.
(10) Shew, C. Y.; Yethiraj, A. Monte-carlo simulations and self-consistent integral equation theory for polyelectrolyte solutions. *J. Chem. Phys.* **1999**, *110*, 5437−5443.
(11) Stevens, M. J.; Kremer, K. Molecular dynamcis simulations of charged polymer chains from dilute to semi dilute concentrations. *ACS Symp. Ser.* **1994**, *548*, 57−66.
(12) Liao, Q.; Dobrynin, A. V.; Rubinstein, M. Counterion-correlation-induced attraction and necklace formation in polyelectrolyte solutions: Theory and simulations. *Macromolecules* **2006**, *39*, 1920−1938.
(13) Liao, Q.; Dobrynin, A. V.; Rubinstein, M. Molecular dynamics simulations of polyelectrolyte solutions: Nonuniform stretching of chains and scaling behavior. *Macromolecules* **2003**, *36*, 3386−3398.

DOI: 10.1021/acs.jpcb.5b01700
J. Phys. Chem. B 2015, 119, 11010−11018

(14) Liao, Q.; Dobrynin, A. V.; Rubinstein, M. Molecular dynamics simulations of polyelectrolyte solutions: Osmotic coefficient and counterion condensation. *Macromolecules* **2003**, *36*, 3399−3410.
(15) Liao, Q.; Carrillo, J. M. Y.; Dobrynin, A. V.; Rubinstein, M. Rouse dynamics of polyelectrolyte solutions: Molecular dynamics study. *Macromolecules* **2007**, *40*, 7671−7679.
(16) Chang, R. W.; Yethiraj, A. Solvent effects on the collapse dynamics of polymers. *J. Chem. Phys.* **2001**, *114*, 7688−7699.
(17) Chang, R. W.; Yethiraj, A. Strongly charged flexible polyelectrolytes in poor solvents: Molecular dynamics simulations with explicit solvent. *J. Chem. Phys.* **2003**, *118*, 6634−6647.
(18) Chang, R. W.; Yethiraj, A. Dilute solutions of strongly charged flexible polyelectrolytes in poor solvents: Molecular dynamics simulations with explicit solvent. *Macromolecules* **2006**, *39*, 821−828.
(19) Park, S.; Zhu, X.; Yethiraj, A. Atomistic simulations of dilute polyelectrolyte solutions. *J. Phys. Chem. B* **2012**, *116*, 4319−4327.
(20) Molnar, F.; Rieger, J. Like-charge attraction between anionic polyelectrolytes: Molecular dynamics simulations. *Langmuir* **2005**, *21*, 786−789.
(21) Chialvo, A. A.; Simonson, J. M. Solvation behavior of short-chain polystyrene sulfonate in aqueous electrolyte solutions: A molecular dynamics study. *J. Phys. Chem. B* **2005**, *109*, 23031−23042.
(22) Carrillo, J. M. Y.; Dobrynin, A. V. Detailed molecular dynamics simulations of a model NaPSS in water. *J. Phys. Chem. B* **2010**, *114*, 9391−9399.
(23) Marrink, S. J.; de Vries, A. H.; Mark, A. E. Coarse grained model for semiquantitative lipid simulations. *J. Phys. Chem. B* **2004**, *108*, 750−760.
(24) Lee, H.; de Vries, A. H.; Marrink, S. J.; Richard, W. P. A coarse-grained model for polyelethyle oxide and polyethylene glycol: Conformation and hydrodynamics. *J. Phys. Chem. B* **2009**, *113*, 13186−13194.
(25) Choi, E.; Mondal, J.; Yethiraj, A. Coarse-grained models for aqueous polyethyle glycol solutions. *J. Phys. Chem. B* **2014**, *118*, 323−329.
(26) Rossi, G.; Monticelli, L.; Puisto, S. R.; Vattulainen, I.; Ala-Nissila, T. Coarse-graining polymers with the MARTINI force-field: Polystyrene as a benchmark case. *Soft Matter* **2011**, *7*, 698.
(27) Li, C.; Shen, J.; Peter, C.; van der Vegt, N. F. A. A chemically accurate implicit-solvent coarse-grained model for polystyrene sulfonate solutions. *Macromolecules* **2012**, *45*, 2551−2561.
(28) Yesylevskyy, S. O.; Schafer L. V.; Sengupta, D.; Marrink, S. J. Polarizable water model for the coarse-grained MARTINI force field *PLoS Comput. Biol.* **2010**, *6*, Article number: e1000810.
(29) Wu, Z.; Cui, Q.; Yethiraj, A. A new coarse-grained model for water: The importance of electrostatic interactions. *J. Phys. Chem. B* **2010**, *114*, 10524−10529.
(30) Marrink, S. J.; Risselada, H. J.; Yefimov, S.; Tieleman, D. P.; de Vries, A. H. The MARTINI force field: Coarse grained model for biomolecular simulations. *J. Phys. Chem. B* **2007**, *111*, 7812−7824.
(31) Wu, Z.; Cui, Q.; Yethiraj, A. A new coarse-grained force field for membrane-peptide simulations. *J. Chem. Theory Comput.* **2011**, *7*, 3793−3802.
(32) Wu, Z.; Cui, Q.; Yethiraj, A. Driving force for the association of hydrophobic peptides: The importance of electrostatic interactions in coarse grained water models. *J. Phys. Chem. Lett.* **2011**, *2*, 1794−1798.
(33) Wu, Z.; Cui, Q.; Yethiraj, A. Why do arginine and lysine organize lipids differently? Insights from coarse-grained and atomistic simulations. *J. Phys. Chem. B* **2013**, *117*, 12145−12156.
(34) Hess, B.; Kutzner, C.; van der Spoel, D.; Lindahl, E. GROMACS 4: Algorithms for highly efficient, load-balanced, and scalable molecular simulation. *J. Chem. Theory Comput.* **2008**, *4*, 435.
(35) He, X. B.; Guvench, O.; MacKerell, A. D.; Klein, M. L. Atomistic simulation study of linear alkylbenzene sulfonates at the water/air Interface. *J. Phys. Chem. B* **2010**, *114*, 9787−9794.
(36) Darden, T.; York, D.; Pedersen, L. Particle mesh ewald: An Nlog(N) method for Ewald sums in large systems. *J. Chem. Phys.* **1993**, *98*, 10089−10092.
(37) Essmann, U.; Perera, L.; Berkowitz, M. L.; Darden, T.; Lee, H.; Pedersen, L. G. A smooth particle mesh Ewald method. *J. Chem. Phys.* **1995**, *103*, 8577−8593.
(38) Hess, B.; Bekker, H.; Berendsen, H. J. C.; Fraaije, J. LINCS: A linear constraint solver for molecular simulations. *J. Comput. Chem.* **1997**, *18*, 1463−1472.
(39) Nose, S. A unified formulation of the constant temperature molecular dynamics methods. *J. Chem. Phys.* **1984**, *81*, 511−519.
(40) Hoover, W. G. Canonical dynamics: Equilibrium phase-space distributions. *Phys. Rev. A* **1985**, *31*, 1695−1697.
(41) Parrinello, M.; Rahman, A. Polymorphic transitions in single crystals: A new molecular dynamics method. *J. Appl. Phys.* **1981**, *52*, 7182−7190.
(42) Kumar, S.; Rosenberg, J. M.; Bouzida, D.; Swendsen, R. H.; Kollman, P. A. The weighted histogram analysis method for free-energy calculations on biomolecules. I. The method. *J. Comput. Chem.* **1992**, *13*, 1011−1021.
(43) Grossfield, A. WHAM: The weighted histogram analysis method, version 2.0.6, 2012. http://membrane.urmc.rochester.edu/content/wham (accessed May 2015).
(44) Dobrynin, A. V.; Rubinstein, M.; Obukhov, S. P. Cascade of transitions of polyelectrolytes in poor solvents. *Macromolecules* **1996**, *29*, 2974−2979.
(45) Yethiraj, A. Conformational properties and static structure factor of polyelectrolyte solutions. *Phys. Rev. Lett.* **1997**, *78*, 3789−3792.
(46) Yethiraj, A. Liquid state theory of polyelectrolyte solutions. *J. Phys. Chem. B* **2009**, *113*, 1539−1551.
(47) Batzill, A.; Luxemburger, R.; Deike, R.; Weber, A. Structural and dynamical properties of aqueous suspensions of NaPSS (HPSS) at very low ionic strength. *Eur. Phys. J. B* **1998**, *1*, 491−5011.
(48) Spiteri, M. N.; Boue, F.; Lapp, A.; Cotton, J. P. Persistence length for a PSSNa polyion in semidilute solution as a function of the ionic strength. *Phys. Rev. Lett.* **1996**, *77*, 5218−5220.
(49) Spiteri, M.; Boue, F.; Lapp, A.; Cotton, J. P. Polyelectrolyte persistence length in semidilute solution as a function of the ionic strength. *Phys. B* **1997**, *234*, 303−305.
(50) Spiteri, M. N.; Williams, C. E.; Boue, F. Pearl-necklace like chain conformation of hydrophobic polyelectrolyte: A SANS study of partially sulfonated polystyrene in water. *Macromolecules* **2007**, *40*, 6679−6691.
(51) Essafi, W.; Spiteri, C. E.; Williams, C.; Boue, F. Hydrophobic polyelectrolytes in better polar solvent: Structure and chain conformation as seen by SAXS and SANS. *Macromolecules* **2009**, *42*, 9568−9580.
(52) Manning, Gerald S. Limiting laws and counterion condensation in polyelectrolyte solutions I. Colligative properties. *J. Chem. Phys.* **1969**, *51*, 924−933.

DOI: 10.1021/acs.jpcb.5b01700
J. Phys. Chem. B 2015, 119, 11010−11018